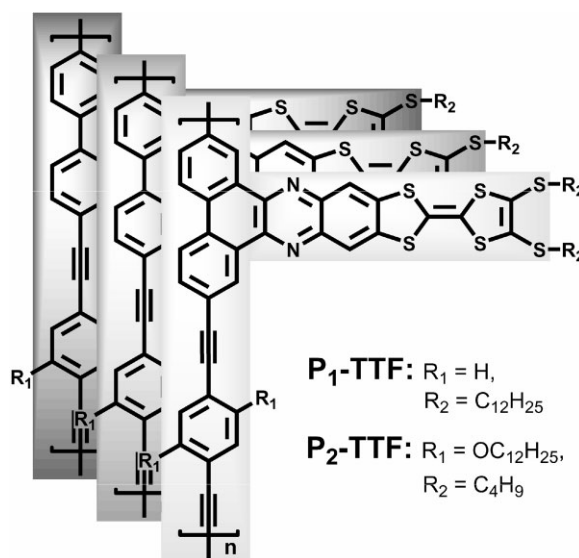


# Semiconducting Oligo-(Aryleneethynylene)s with Coplanarity of Main Chain and Tetrathiafulvalene (TTF) Side Chains: Synthesis, Self-Assembly, and Conductive Properties

Yanhui Hou, Min Yang, Xiangjian Wan, Jie Mao, Yanfeng Ma, Yi Huang, Yongsheng Chen\*

Two oligo-(aryleneethynylene)s, with coplanarity of main chain and tetrathiafulvalene (TTF) side chains, have been prepared and characterized. The X-ray diffractions (XRDs) show that their  $\pi$ -extended coplanar backbones can form continuous  $\pi$ -stacking. For the two oligomers, one stacks in the inter-digitation packing mode; another stacks in the end-to-end packing mode. Cyclic voltammeteries reveal that the two oligomers have almost the same reversible electroactive properties. The TTF units of the two oligomers can be oxidized to  $\text{TTF}^{\bullet 1+}$  by  $\text{Fe}(\text{bpy})_3(\text{PF}_6)_3$  ( $\text{bpy} = 2,2'$ -bipyridine). The band gaps, deduced from UV-Vis absorption spectra, are 1.92 and 2.03 eV, respectively. The conductivities of the two oligomers are  $1 \times 10^{-5}$  and  $6 \times 10^{-8} \text{ S} \cdot \text{cm}^{-1}$  at room temperature. The charge transfer (CT) complexes of the oligomers and tetracyanoquinodimethane (TCNQ) exhibit higher conductivity up to  $0.2 \text{ S} \cdot \text{cm}^{-1}$ .



## Introduction

Since the discovery of high conductivity in doped polyacetylene samples three decades ago,<sup>[1]</sup>  $\pi$ -conjugated polymers have attracted great interest for their unique electronic properties.<sup>[2,3]</sup> Because the electronic properties of conjugated polymers sensitively depend on their molecular structures, a lot of conjugated polymers with different main chains and various substituents have been synthesized for different applications.<sup>[4,5]</sup> In addition, tetrathiafulvalene (TTF) and its derivatives are well-known for their unique electron-donating property and reversible electroactivity.

Y. Hou

School of Materials Science and Chemical Engineering, Tianjin Polytechnic University, Tianjin 300160, China

X. Wan, J. Mao, Y. Ma, Y. Huang, Y. Chen

Key Laboratory for Functional Polymer Materials and Centre for Nanoscale Science and Technology, Institute of Polymer Chemistry, College of Chemistry, Nankai University, Tianjin 300071, China

Fax: (+86) 22 23499992; E-mail: yscheng99@nankai.edu.cn

M. Yang

Institute of Polymer Science and Engineering, Hebei University of Technology, Tianjin 300130, China

They were often used in the metallic charge transfer (CT) complexes as the donors.<sup>[6–8]</sup> So the concept of combining TTF with linear  $\pi$ -conjugated polymers offers exciting potentialities to develop original organic conducting materials.<sup>[9]</sup> From the viewpoint of polymer physical properties, polymers are well known for their good film-forming property. The association of TTF units with linear  $\pi$ -conjugated polymers could overcome the brittle and unprocessable properties of the CT complexes.<sup>[10–12]</sup> Moreover, for the conjugated polymers with TTF units, a charge conducting path can be formed not only along the main chains of the polymers via  $\pi$ -conjugation, the self-assembly regular stacking of TTF units might also form another conducting pathway via inter-molecular  $\pi$ -orbital overlap.<sup>[9–13]</sup> Furthermore, the TTF polymer constitutes a highly polarizable species due to the large number of sulfur atoms in the structure. Thus, the extended conjugation could decrease the intra-molecular Coulomb repulsive energy between the donor units, and enhance intra-molecular and inter-stack interactions and further enhance conductivity of these materials.<sup>[10,14]</sup>

There are many reports about preparing the conjugated polymers with TTF units either in the main chains or in the side chains.<sup>[10,15]</sup> For some TTF polymers, the strong propensity of TTFs to self-assemble into regular  $\pi$ -stacking is an interesting approach for indirectly controlling the long-range order of the conjugated chains. However, for most of the reported TTF polymers, the TTF units and the polymer skeletons can give rise to a lot of possible conformations. Especially, for the polymers with TTF side chains, it is difficult to achieve the coplanarity of main chains and TTF side chains, so the whole molecules couldn't form continuous stacking.<sup>[15]</sup> Recently, we preliminary report a novel oligo-(*p*-aryleneethynylene) with coplanarity of main chain and TTF side chains, in which the  $\pi$ -conjugated TTF units attach to the planar main chain by the conjugated phenazine rings.<sup>[16]</sup> As expected, the  $\pi$ -extended coplanar backbones of the oligomer could form good continuous stacking in the solid state. If tetracyanoquinodimethane (TCNQ) is added to the TTF polymers, the CT between the TTF units and TCNQ will make the conducting pathway of the TTF units' stacking become completely through, and the conductivity of the polymer will increase a lot. As a part of the continuous work, two oligomers were synthesized. The CT complexes of the two oligomers and TCNQ were also obtained. Herein we describe the preparation, self-assembly, and electroactive characterization of the two oligomers. The conductive properties of the oligomers and the complexes are also discussed.

## Experimental Part

### Measurements

<sup>1</sup>H NMR spectra were recorded on a Bruker AC-300 Spectrometer. Mass spectra (MS) were recorded using a Thermofinnigan LCQ

Advantage mass spectrometer. Elemental analyses were performed on a Thermo Electron FLASH/EA 1112 instrument. Gel permeation chromatography (GPC) analysis was conducted on Polymer Lab PL-220 using polystyrene as standard. FT-IR spectra were recorded on Bruker Vector-22 spectrometer. Thermogravimetric analysis (TGA) measurements were performed on a TA instrument SDT-TG Q600 under nitrogen atmosphere at a heating rate of 10 °C · min<sup>-1</sup>. Differential scanning calorimetry (DSC) measurements were recorded on a TA instrument DSC-2910 under an atmosphere of N<sub>2</sub> at a heating rate of 10 °C · min<sup>-1</sup>. X-ray diffraction (XRD) were performed with a Rigaku X-ray diffractometer (D/max-2500). UV-Vis spectra were recorded on a JASCO-V570 spectrometer. Cyclic voltammetry (CV) measurements were performed on a LK98B II Microcomputer-based Electrochemical Analyze at room temperature with a three-electrode cell in a solution of Bu<sub>4</sub>NPF<sub>6</sub> (0.1 M) in acetonitrile at a scanning rate of 100 mV · s<sup>-1</sup>. A platinum wire was used as a counter electrode, and an Ag/AgNO<sub>3</sub> electrode was used as a reference electrode. After measurement the reference electrode was calibrated with ferrocene (Fc) and the potential axis was corrected to Fc/Fc<sup>+</sup>. The conductivities of the oligomers were conducted on a computer controlled Keithley 2400 source measure unit. Electron paramagnetic resonance (EPR) studies were performed with a Bruker EMX-6/1 spectrometer.

### Materials

Unless stated otherwise, all chemicals and reagents were purchased reagent-grade and used without further purification. Air and/or water-sensitive reactions were conducted under nitrogen using dry, freshly distilled solvents. The synthesis of 5,6-diamino-2-[4,5-bis(alkylthio)-1,3-dithiole-2-ylidene]benzo[d]-1,3-dithioles (**3<sub>a,b</sub>**), 2,7-diiodophenanthrene-9,10-dione (**4**), 1,4-diethynylbenzene (**6**), 1,4-bis[dodecyloxy]-2,5-diethynylbenzene (**7**) and Fe(bpy)<sub>3</sub>(PF<sub>6</sub>)<sub>3</sub> (bpy = 2,2'-bipyridine) were prepared according to the literature procedures.<sup>[16–21]</sup>

### Monomer Synthesis

#### 4',5'-Bis(dodecylthio)tetrathiafulvenyl-2,7-diiondibenzo[a,c]phenazine (**5<sub>a</sub>**)

The mixture of compound **3<sub>a</sub>** (0.343 g, 0.5 mmol) and **4** (0.23 g, 0.5 mmol) in 60 mL ethanol was refluxed for 3 h under N<sub>2</sub> and protected from light. After filtration, the precipitate was collected and purified by chromatography (basic Al<sub>2</sub>O<sub>3</sub>, CH<sub>2</sub>Cl<sub>2</sub>) to give **5<sub>a</sub>** as a deep blue solid (0.377 g, 68%). <sup>1</sup>H NMR (300 M, *o*-C<sub>6</sub>D<sub>4</sub>Cl<sub>2</sub>):  $\delta$  = 9.27 (s, 2H), 9.02 (d, *J* = 8.1 Hz, 2H), 8.28 (d, *J* = 8.1 Hz, 2H), 8.06 (s, 2H), 2.81 (t, *J* = 7.3 Hz, 4H), 1.61 (m, 4H), 1.24 (m, 36H), 0.86 (t, *J* = 7.3 Hz, 6H). APCI-MS (*m/z*), 1108.9 (M+H<sup>+</sup>). Elemental analysis calcd for C<sub>48</sub>H<sub>58</sub>I<sub>2</sub>N<sub>2</sub>S<sub>6</sub>: C, 51.98; H, 5.27; N, 2.53; S, 17.35%. Found: C, 52.05; H, 5.33; N, 2.58; S, 17.42%.

#### 4',5'-Bis(butylthio)tetrathiafulvenyl-2,7-diiondibenzo[a,c]phenazine (**5<sub>b</sub>**)

By following similar procedure above, **4** and **3<sub>b</sub>** were used to give **5<sub>b</sub>** as a deep blue solid (yield 70%). <sup>1</sup>H NMR (300 M, *o*-C<sub>6</sub>D<sub>4</sub>Cl<sub>2</sub>):  $\delta$  = 9.30

(s, 2H), 9.05 (d,  $J = 8.1$  Hz, 2H), 8.29 (d,  $J = 8.1$  Hz, 2H), 8.06 (s, 2H), 2.81 (t,  $J = 7.1$  Hz, 4H), 1.52 (m, 4H), 1.35 (m, 4H), 0.84 (t,  $J = 7.3$  Hz, 6H). APCI-MS ( $m/z$ ), 885.4 ( $M+H^+$ ). Elemental analysis calcd for  $C_{32}H_{26}I_2N_2S_6$ : C, 43.44; H, 2.96; N, 3.17; S, 21.74%. Found: C, 43.38; H, 3.01; N, 3.11; S, 21.82%.

## Polymer Synthesis

### Oligomer $P_1$ -tetrathiafulvalene ( $P_1$ -TTF)

Diisopropylamine (2 mL) was added to a mixture of compound **5<sub>a</sub>** (0.111 g, 0.1 mmol), **6** (0.013 g, 0.1 mmol), Pd(PPh<sub>3</sub>)<sub>4</sub> (0.012 g, 0.01 mmol) and CuI (0.002 g, 0.01 mmol) in 30 mL THF under an argon atmosphere. The mixture was refluxed for 48 h. After being cooled to room temperature, the solid was collected by filtration and dissolved in as little 1,2,4-trichlorobenzene as possible. The solution was poured into DMF to give the desired  $P_1$ -TTF precipitate, which was separated by filtration and washed with methanol thoroughly. (0.076 g, 74%) <sup>1</sup>H NMR (300 M, *o*-C<sub>6</sub>D<sub>4</sub>Cl<sub>2</sub>):  $\delta = 9.29$  (s, 2H), 9.01 (d,  $J = 8.1$  Hz, 2H), 8.26 (d,  $J = 8.1$  Hz, 2H), 8.04 (s, 2H), 7.62 (d, 4H), 2.83 (m, 4H), 1.96 (m, 4H), 1.26 (br, 36H), 0.92 (m, 6H). GPC (eluent: 1,2,4-trichlorobenzene):  $\bar{M}_n = 7500$ ,  $\bar{DP} = 7$ , PDI = 2.1. Elemental analysis calcd for (C<sub>58</sub>H<sub>62</sub>N<sub>2</sub>S<sub>6</sub>)<sub>*n*</sub>: C, 71.12; H, 6.38; N, 2.86; S, 19.64%. Found: C, 70.73; H, 6.17; N, 3.02; S, 20.21%.

### Oligomer $P_2$ -tetrathiafulvalene ( $P_2$ -TTF)

The reaction was carried out by following the procedure above. After the reaction, the resulting solution was poured into DMF. The precipitated solid was re-dissolved in THF and re-precipitated in DMF for two times. The product  $P_2$ -TTF was separated by filtration and washed with a lot of methanol, and dried under vacuum (yield: 71%). <sup>1</sup>H NMR (300 M, CDCl<sub>3</sub>):  $\delta = 9.32$  (s, 2H), 9.06 (d,  $J = 8.2$  Hz, 2H), 8.33 (d,  $J = 8.2$  Hz, 2H), 8.04 (s, 2H), 6.98 (s, 2H), 2.81 (m, 8H), 1.66 (br, 8H), 1.26 (br, 40H), 0.88 (m, 12H). GPC (eluent: THF):  $\bar{M}_n = 13000$ ,  $\bar{DP} = 12$ , PDI = 1.6. Elemental analysis calcd for (C<sub>66</sub>H<sub>78</sub>N<sub>2</sub>O<sub>2</sub>S<sub>6</sub>)<sub>*n*</sub> (1122.5)<sub>*n*</sub>: C, 70.54; H, 7.00; N, 2.49; S, 17.12%. Found: C, 69.93; H, 6.79; N, 2.96; S, 17.85%.

### Chemical Oxidization of $P_1$ -tetrathiafulvalene and $P_2$ -tetrathiafulvalene

Excess of solid Fe(bpy)<sub>3</sub>(PF<sub>6</sub>)<sub>3</sub> was added to the solutions of  $P_1$ -TTF,  $P_2$ -TTF in *o*-dichlorobenzene under N<sub>2</sub>, respectively. The mixtures

were stirred at room temperature under dark for 1 h. After filtration, the  $P_1$ -TTF<sup>•1+</sup> and  $P_2$ -TTF<sup>•1+</sup> solutions were obtained, which were immediately used in the EPR and UV-Vis spectra measurements.

### Synthesis of Adducts $P_1$ -tetrathiafulvalene/tetracyanoquinodimethane ( $P_1$ -TTF/TCNQ) and $P_2$ -tetrathiafulvalene/tetracyanoquinodimethane ( $P_2$ -TTF/TCNQ)

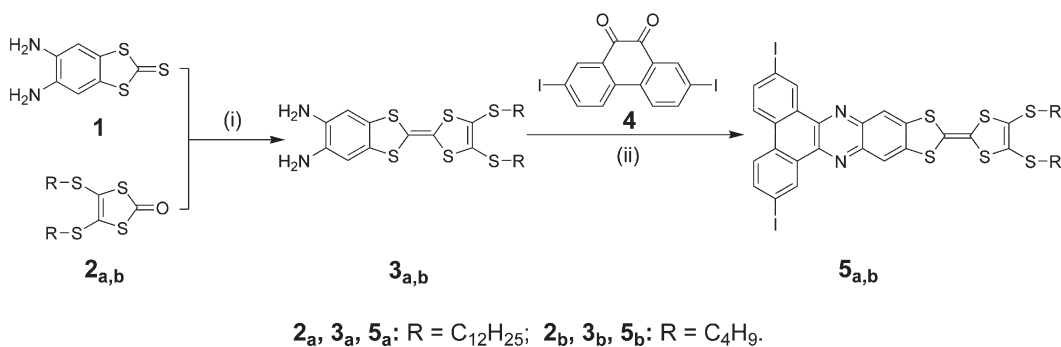
For the desired CT complexes with different donor/acceptor ratios, different amounts of solid TCNQ were added to the saturated solutions of  $P_1$ -TTF and  $P_2$ -TTF in 1,2,4-trichlorobenzene, respectively. The mixtures were stirred at room temperature for 1 h. After reaction, ethanol was added into the mixtures. The precipitated solids were separated by filtration and washed with ethanol, and dried under vacuum to give the CT complexes. For  $P_1$ -TTF/TCNQ with 1:2 molar ratio of TTF units/TCNQ [(C<sub>32</sub>H<sub>70</sub>N<sub>10</sub>S<sub>6</sub>)<sub>*n*</sub>], elemental analysis calcd: C, 70.96; H, 5.08; N, 10.09; S, 13.86%. Found: C, 71.08; H, 5.11; N, 9.98; S, 13.92%. For  $P_2$ -TTF/TCNQ with 1:2 molar ratio of TTF units/TCNQ [(C<sub>90</sub>H<sub>86</sub>N<sub>10</sub>O<sub>2</sub>S<sub>6</sub>)<sub>*n*</sub>], elemental analysis calcd: C, 70.55; H, 5.66; N, 9.14; S, 12.56%. Found: C, 70.63; H, 6.54; N, 9.08; S, 12.95%.

## Results and Discussion

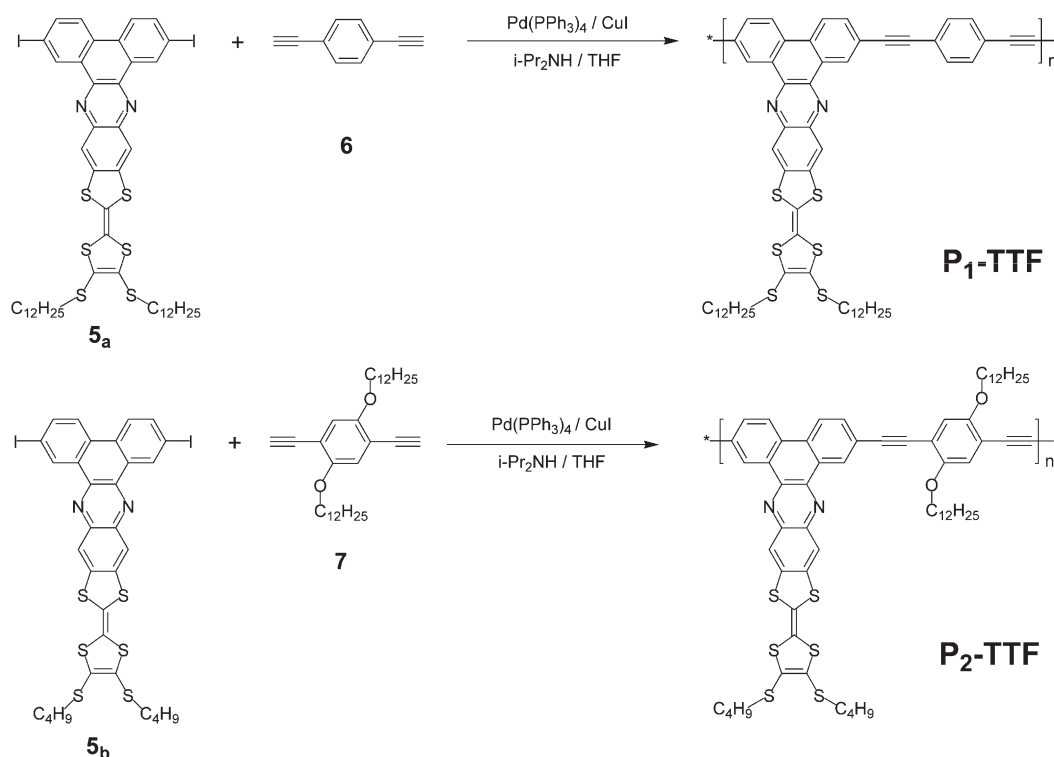
### Synthesis and Characterizations

The synthetic pathway for the monomers **5<sub>a</sub>**, **5<sub>b</sub>** is outlined in Scheme 1. The starting materials **1**, **2<sub>a</sub>**, **2<sub>b</sub>**, **4**, and monomers **6**, **7** were synthesized according to the literatures.<sup>[16–21]</sup> All compounds were purified by chromatographic separation and have been fully characterized.

The oligomers  $P_1$ -TTF,  $P_2$ -TTF were synthesized through Pd-Cu-catalyzed Sonogashira coupling reactions (Scheme 2). After purification and drying, deep-blue  $P_1$ -TTF and brown  $P_2$ -TTF were obtained.  $P_1$ -TTF is insoluble in tetrahydrofuran (THF) and CHCl<sub>3</sub>, but it could be dissolved in *o*-dichlorobenzene and has a relatively good solubility in 1,2,4-trichlorobenzene.  $P_2$ -TTF has a very good solubility in common solvents (such as THF, CHCl<sub>3</sub>, *o*-dichlorobenzene, 1,2,4-trichlorobenzene, etc.). Very interestingly, we found that after the  $P_2$ -TTF THF solution was kept in the dark for



■ Scheme 1. Synthesis routes of the monomers: (i) P(OEt)<sub>3</sub>, toluene, 120 °C, 3 h; (ii) ethanol, reflux, 3 h.



■ Scheme 2. Synthesis routes of **P<sub>1</sub>-TTF** and **P<sub>2</sub>-TTF**.

five days, there was a solid appearing in the solution. Confirmed by the <sup>1</sup>H NMR spectrum, the precipitated solid was still **P<sub>2</sub>-TTF**, and it could be re-dissolved in THF by ultrasonification. Since the main chain and TTF side chains are coplanar, we suspect that the molecules of **P<sub>2</sub>-TTF** realigned slowly in the solution, and the coplanar  $\pi$ -extended backbone of **P<sub>2</sub>-TTF** formed the good  $\pi$ - $\pi$  stacking, which result in the precipitation. This was confirmed by XRD patterns of **P<sub>2</sub>-TTF** (see below). The average molecular weights of **P<sub>1</sub>-TTF** and **P<sub>2</sub>-TTF** were estimated by GPC with polystyrene as calibration standard. Because of the poor solubility of **P<sub>1</sub>-TTF** in THF, 1,2,4-trichlorobenzene was chose as the eluent for **P<sub>1</sub>-TTF**. Data from GPC and the yields are presented in Table 1.

The thermal stabilities of the two oligomers were investigated by TGA under inert nitrogen atmosphere. The TGA analysis revealed that the onset temperatures of

the weight loss of **P<sub>1</sub>-TTF**, **P<sub>2</sub>-TTF** were all about 230 °C. It is obvious that both oligomers exhibit good thermal stability. DSC measurements of the oligomers were also conducted in the inert nitrogen atmosphere. There is no thermal transition observed below 230 °C for the two oligomers, indicating that their molecules are so rigid that the *T<sub>g</sub>* may be higher than the decomposition temperature.

### Electroactive Properties

The electroactive properties of the two oligomers were investigated by CV. Figure 1 shows the cyclic voltammograms of their thin-films on a Pt electrode in a 0.1 M Bu<sub>4</sub>NPF<sub>6</sub> acetonitrile solution. The results of the electrochemical measurements are summarized in Table 2. Obviously, the two oligomers have almost the same redox behavior. The two quasi-reversible single-electron oxidation waves at about 0.5 and 0.77 V are the typical redox peaks of the TTF unit, corresponding to its *E*<sub>ox1</sub> and *E*<sub>ox2</sub>.<sup>[22–24]</sup> The first oxidation is attributed to the bis(thioether)-substituted half-unit of TTF, whilst the second arises from the phenazinedithiol TTF moiety. This assignment is justified by the electron withdrawing effect of the TTF-fused phenazine.<sup>[23]</sup> Moreover, the two oligomers have a quasi-reversible reduction process at about –1.76 V, which could be assigned to the reduction of the electron-withdrawing phenazine moieties and C≡C groups.<sup>[24–26]</sup> The redox

■ Table 1. Results of polymerization.

Polymer	$\overline{M}_n$	$\overline{M}_w$	PDI	$\overline{DP}$	Yield
	$\text{g} \cdot \text{mol}^{-1}$	$\text{g} \cdot \text{mol}^{-1}$			
<b>P<sub>1</sub>-TTF</b>	7 500 <sup>a)</sup>	15 800	2.1	7	74
<b>P<sub>2</sub>-TTF</b>	11 100 <sup>b)</sup>	17 400	1.6	10	87

<sup>a)</sup>1,2,4-trichlorobenzene as the eluent; <sup>b)</sup>THF as the eluent.

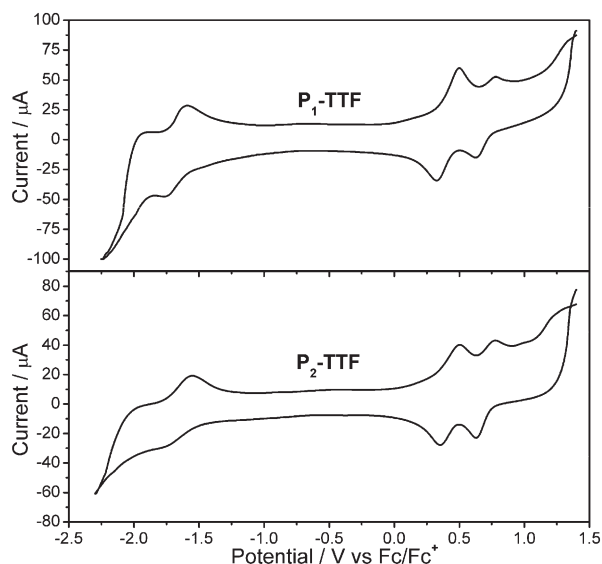


**Figure 1.** Cyclic voltammograms of  $P_1$ -TTF and  $P_2$ -TTF films on platinum plates in acetonitrile solution of 0.1 M  $Bu_4NPF_6$ , with a potential scanning rate of  $0.1 \text{ V} \cdot \text{s}^{-1}$  at room temperature and potential versus  $Fc/Fc^+$ .

properties of  $P_1$ -TTF and  $P_2$ -TTF are similar to that of other similar TTF-fused donor-acceptor (D-A) ensembles. For all the redox processes, their anodic/cathodic peak separation ( $\Delta E_p$ ) should ideally be zero for a surface reaction. However, the measured  $\Delta E_p$  values are about 160 mV. Roncali and coworkers<sup>[27]</sup> suggested the reason was that the redox processes were partially limited by charge and/or mass transformation in the polymer film.

Chemical oxidations of  $P_1$ -TTF and  $P_2$ -TTF were performed by  $Fe(bpy)_3(PF_6)_3$ . After addition of  $Fe(bpy)_3(PF_6)_3$  to the solutions of two oligomers, a sharp signal with  $g = 2.005$  showed up in the EPR spectra (Figure 2). They are in line with the characteristic EPR signal of the cation radical  $TTF^{\bullet 1+}$  units.<sup>[14,28]</sup> Thus we believe that the oxidation of  $P_1$ -TTF and  $P_2$ -TTF generated the radical cations,  $P_1$ -TTF $^{\bullet 1+}$ , and  $P_2$ -TTF $^{\bullet 1+}$ , as outlined in Figure 2. At the same time, these also indicate that the first oxidation wave of  $P_1$ -TTF and that of  $P_2$ -TTF in their CVs happen on the TTF units of the two oligomers.

**Table 2.** Electrochemical characteristics of  $P_1$ -TTF and  $P_2$ -TTF.

Polymer	<i>n</i> -doping	<i>p</i> -doping (first process)	<i>p</i> -doping (second process)
	$E_{red}(V)^a$	$E_{ox1}(V)^a$	$E_{ox2}(V)^a$
$P_1$ -TTF	-1.76	0.50	0.77
$P_2$ -TTF	-1.76	0.50	0.77

<sup>a</sup>)  $E_{ox}$  and  $E_{red}$  values are the peak values.

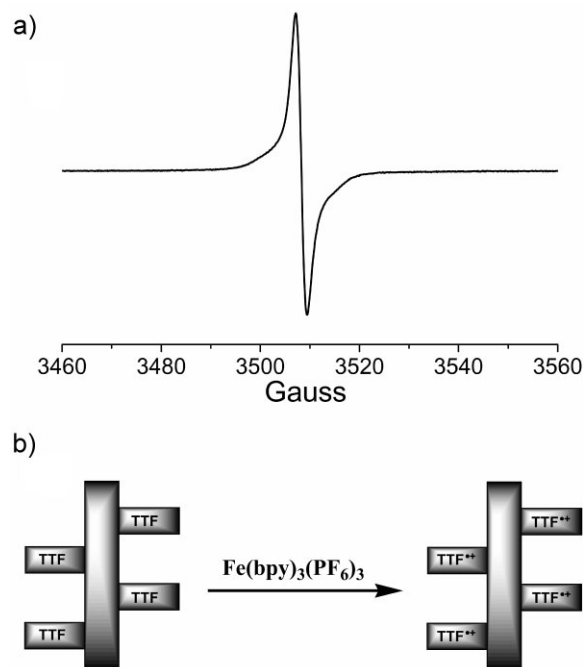


**Figure 2.** (a) EPR spectrum of  $P_1$ -TTF in *o*-dichlorobenzene solution at room temperature (EPR spectrum of  $P_2$ -TTF is the same as that of  $P_1$ -TTF, so it is not showed); (b) cartoon representation of the chemical oxidation of the two oligomers by  $Fe(bpy)_3(PF_6)_3$ .

## Optical Properties

The UV-Vis absorption spectra of  $P_1$ -TTF,  $P_2$ -TTF solutions in *o*-dichlorobenzene and those of their films on quartz plate are shown in Figure 3. In the visible region,  $P_1$ -TTF has one absorption peak at 530 nm and a shoulder peak at  $\approx 380$  nm, and  $P_2$ -TTF has two absorption peaks, which are located at 520 and 400 nm, respectively. The absorptions in the visible region corresponds to the  $\pi$ - $\pi^*$  transition of the conjugated backbones.<sup>[29,30]</sup> In comparison with the absorption spectra of the oligomers solutions, those of their films in the visible region become bathochromically shifted by about 20 nm. This long wavelength band shift indicates the formation of J-aggregates. There exists the offset stacking between the polymer backbones in the films,<sup>[31]</sup> which is consistent with the XRD results (see below). The optical band-gaps ( $E_g^{opt}$ ) of  $P_1$ -TTF,  $P_2$ -TTF are 1.92 and 2.03 eV, estimated from their absorption edges.

The UV-Vis absorption spectra of  $P_1$ -TTF $^{\bullet 1+}$ ,  $P_2$ -TTF $^{\bullet 1+}$  solutions in *o*-dichlorobenzene are also shown in Figure 3. After oxidation by  $Fe(bpy)_3(PF_6)_3$ , there appears a new broad absorption between 700 and 1 000 nm, which is the characteristic absorption of the cation radical  $TTF^{\bullet 1+}$ .<sup>[22-24]</sup>

## X-Ray Diffraction

X-ray diffraction (XRD) patterns of  $P_1$ -TTF and  $P_2$ -TTF are shown in Figure 4. Note that the XRD for  $P_2$ -TTF before and

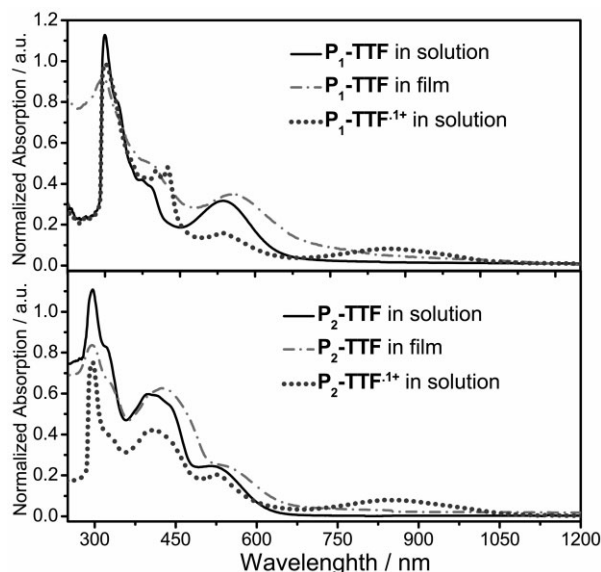


**Figure 3.** UV-Vis absorption spectra of  $P_1$ -TTF,  $P_2$ -TTF,  $P_1$ -TTF<sup>1+</sup>, and  $P_2$ -TTF<sup>1+</sup> solutions in *o*-dichlorobenzene, and that of  $P_1$ -TTF,  $P_2$ -TTF film on quartz plates.  $P_1$ -TTF<sup>1+</sup> and  $P_2$ -TTF<sup>1+</sup> solutions were obtained by chemical oxidation of  $P_1$ -TTF,  $P_2$ -TTF by Fe(bpy)<sub>3</sub>(PF<sub>6</sub>)<sub>3</sub>.

after the slow re-precipitation from its THF solution are both shown. The strong reflections at low angles together with their higher orders indicate that both the polymers could form layered order structures in which the rigid-rod main chains are separated by the alkyl side chains. The  $d$  values were derived using the Bragg law  $2d \sin\theta = n\lambda$ , where  $n$ ,  $\lambda$ , and  $\theta$  denote the order of the diffraction, wavelength of an X-ray beam, and Bragg angle, respectively. The diffraction peak  $d_1$  is assigned to the side-to-side distance between the conjugated main chains separated by the long side chains, as reported from those of other similar  $\pi$ -conjugated polymers with long side chains.<sup>[32–35]</sup> The  $d_2$  peak is assigned to the second-order peak of  $d_1$  ( $d_2 = d_1/2$ ). Note the alkyl chains on the TTF units of  $P_1$ -TTF are longer than that of  $P_2$ -TTF. However, the  $d_1$  value (35.31 Å) of  $P_1$ -TTF is less than that of  $P_2$ -TTF (38.38 Å). A reasonable explanation is that the long dodecyl chains on the TTF units of  $P_1$ -TTF take the inter-digitation packing mode (Figure 5). Whereas, because the dodecyloxy chains on the main chain of  $P_2$ -TTF take the space between the butyl chains on the TTF units, the short butyl chains on the TTF units of  $P_2$ -TTF couldn't form the inter-digitation packing mode like that of  $P_1$ -TTF, and only take the end-to-end packing mode (Figure 6). In addition, the

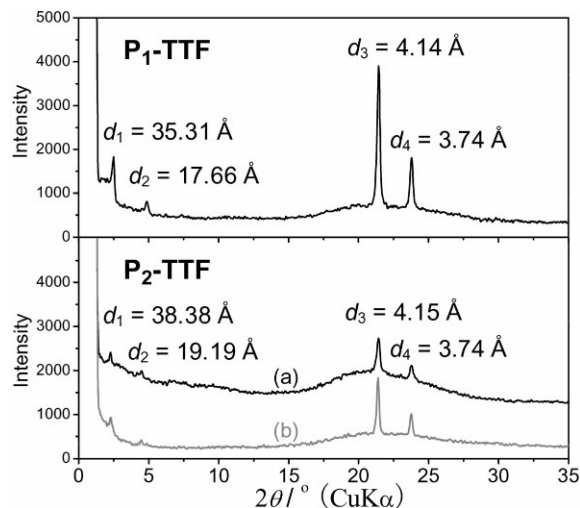


**Figure 4.** XRD patterns of the powder of  $P_1$ -TTF, the powder of  $P_2$ -TTF (a), and the realigned solid of  $P_2$ -TTF (b), which was slowly precipitated from the THF solution. Peaks are labeled with  $d$ -spacing in angstroms.

length of the rigid portion of the side chain is about 15 Å. Adding the short butyl chains, the total length of the side chain is about 19 Å, which also approves that  $P_2$ -TTF take the end-to-end packing mode.

Since the effective cross-section of the alkyl chains is about  $S = 20 \text{ Å}^2$ , their hexagon-like aggregation give about  $d = 4.2 \text{ Å}$ .<sup>[34]</sup> This value is in agreement with what we observed for the peak at  $d_3$  from the oligomers, as shown in Figure 4. The value of  $d_4$  is very close to the  $\pi$ -stacking distances of reported TTF-fused D-A organic compounds, which were observed from their single crystal structures.<sup>[22,36,37]</sup> So  $d_4$  is considered to be the offset stacking

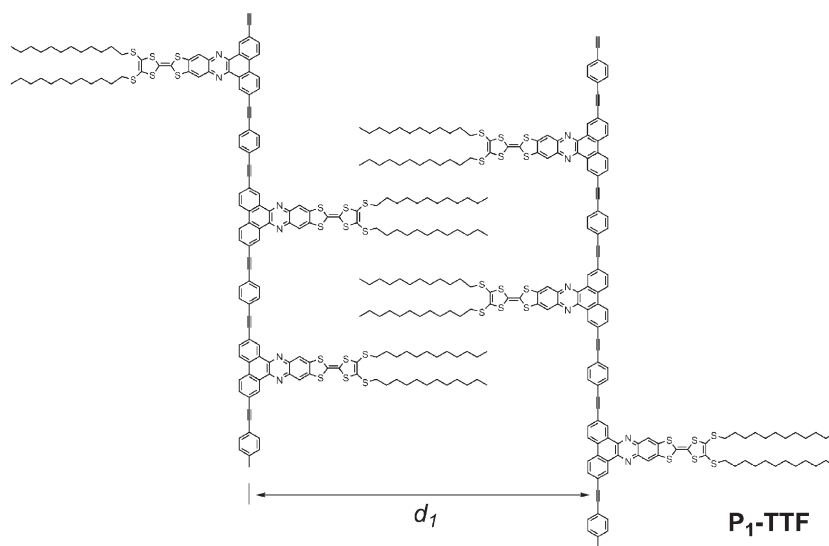


**Figure 5.** Schematic representation of an inter-digitation packing mode of  $P_1$ -TTF in solid state.

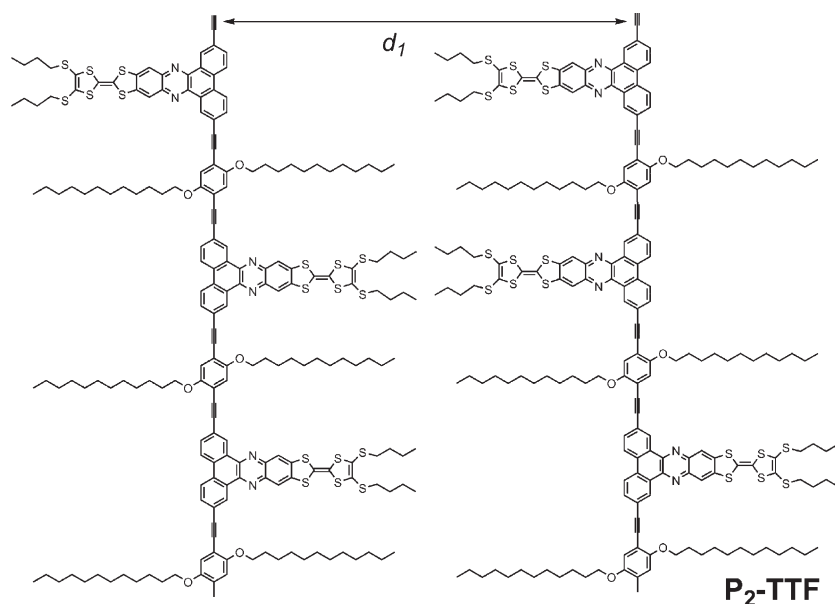


Figure 6. Schematic representation of an end-to-end packing mode of the realigning solid of  $P_2$ -TTF.

distance between the coplanar backbones. Obviously, the two oligomers formed ordered structures in the solid state due to the stacking of the  $\pi$ -extended coplanar backbones and the crystallinity of the long alkyl chains.

Moreover, since the peaks of  $P_1$ -TTF are much sharper than that of  $P_2$ -TTF,  $P_1$ -TTF molecules are believed to pack in a better ordered structure in the solid state. The long alkoxy chains on the main chain of  $P_2$ -TTF might inhibit more the  $\pi$ -stacking of the backbones. But for  $P_2$ -TTF, by slowly realigning in THF solution, the amorphous phase diminished a lot, as observed from the enhanced XRD peaks in Figure 4.

### Conductivity Measurements

Because of the good continuous stacking of  $P_1$ -TTF and  $P_2$ -TTF, we expect that the two oligomers have good electronic properties. So the conductivity measurements by four-probe methods were performed on compress pellets of the two oligomers at room temperature. The conductivities of the powders of  $P_1$ -TTF and  $P_2$ -TTF are  $1 \times 10^{-5}$  and  $6 \times 10^{-8} \text{ S} \cdot \text{cm}^{-1}$ . Obviously,  $P_2$ -TTF has poorer conductivity than  $P_1$ -TTF. However, by slowly re-precipitating from its THF solution, the conductivity of  $P_2$ -TTF increases to  $4 \times 10^{-6} \text{ S} \cdot \text{cm}^{-1}$ .  $P_2$ -TTF has better ordered-structure after realigning in the solution, which results in the improvement of the conductivity.

The two oligomers reacted with electron acceptor TCNQ in 1,2,4-trichlorobenzene solutions to give CT adducts. Among these adducts, the CT complex of  $P_1$ -TTF/TCNQ (1:2 molar ratio of TTF units/TCNQ) shows the maximum

conductivity of  $0.2 \text{ S} \cdot \text{cm}^{-1}$  as measured on the compressed pellet of the complex. The conductivity of  $P_2$ -TTF/TCNQ (1:2 molar ratio of TTF units/TCNQ) is  $0.07 \text{ S} \cdot \text{cm}^{-1}$ . The interesting results should come from the increase in dimensionality of the conduction process. For the neutral TTF-fused oligomers, charge conduction is only along the conjugated backbone. However, when TTF units form the CT complex with TCNQ, the  $\pi$ -orbital overlap stacking of TTF units also become the conducting pathway.

### Conclusion

To summarize, we have prepared two novel TTF-fused oligo-(aryleneethynylene)s with coplanarity of main chain and TTF side chains. They reveal good reversible electroactivity. The coplanarity of the main chain and the donor TTF side

chains ensure that the oligomers can form continuous  $\pi$ -stacking in the solid state and show semiconductivity. So when the oligomers formed the CT complexes with TCNQ, the  $\pi$ -orbital overlap stacking of TTF units also become the conducting pathway. The continuous stacking and reversible electroactive properties indicate that this kind of TTF-fused oligomers may become a promising active material for organic electronic applications.

Acknowledgements: We gratefully acknowledge the financial support from the NSFC (no. 20644004, no. 20774047), MoST (no. 2006CB932702), NSF of Tianjin City (no. 07JCYBJC03000) and the Startup Fund for PhDs of Natural Scientific Research of Tianjin Polytechnic University (no. 029312).

Received: February 18, 2009; Revised: April 18, 2009; Accepted: April 21, 2009; DOI: 10.1002/macp.200900070

Keywords: conducting polymers; coplanarity; self-assembly;  $\pi$ -stacking; tetrathiafulvalene

- [1] H. Shirakawa, E. J. Louis, A. G. MacDiarmid, C. K. Chiang, A. J. Heeger, *J. Chem. Soc., Chem. Commun.* **1977**, 578.
- [2] J. Roncali, P. Leriche, A. Cravino, *Adv. Mater.* **2007**, *19*, 2045.
- [3] M. Kertesz, C. H. Choi, S. Yang, *Chem. Rev.* **2005**, *105*, 3448.
- [4] C. Li, Y. Li, *Macromol. Chem. Phys.* **2008**, *209*, 1541.
- [5] S. Günes, H. Neugebauer, N. S. Sariciftci, *Chem. Rev.* **2007**, *107*, 1324.

- [6] M. Bendikov, F. Wudl, D. F. Perepichka, *Chem. Rev.* **2004**, *104*, 4891.
- [7] A. Gorgues, P. Hudhomme, M. Sallé, *Chem. Rev.* **2004**, *104*, 5151.
- [8] M. Fourmigué, P. Batail, *Chem. Rev.* **2004**, *104*, 5379.
- [9] L. Huchet, S. Akoudad, J. Roncali, *Adv. Mater.* **1998**, *10*, 541.
- [10] S. Inagi, K. Naka, Y. Chujo, *J. Mater. Chem.* **2007**, *17*, 4122.
- [11] T. Uemura, K. Naka, Y. Chujo, *Adv. Polym. Sci.* **2004**, *167*, 81.
- [12] J. L. Segura, N. Martín, *Angew. Chem., Int. Ed.* **2001**, *40*, 1372.
- [13] M. Adam, K. Müllen, *Adv. Mater.* **1994**, *6*, 439.
- [14] F. Wudl, *Acc. Chem. Res.* **1984**, *17*, 227.
- [15] E. Gomar-Nadal, L. Mugica, J. Vidal-Gancedo, J. Casado, J. T. L. Navarrete, J. Veciana, C. Rovira, D. B. Amabilino, *Macromolecules* **2007**, *40*, 7521.
- [16] Y. Hou, Y. Chen, Q. Liu, M. Yang, X. Wan, M. Yang, S. Yin, A. Yu, *Macromolecules* **2008**, *41*, 3114.
- [17] M. Frei, F. Diederich, R. Tremont, T. Rodriguez, L. Echegoyen, *Helv. Chim. Acta* **2006**, *89*, 2040.
- [18] P. Luliński, L. Skulski, *Bull. Chem. Soc. Jpn.* **1999**, *72*, 115.
- [19] M. J. Plater, J. P. Sinclair, S. Aiken, T. Gelbrich, M. B. Hursthouse, *Tetrahedron* **2004**, *60*, 6385.
- [20] Q. Fang, S. Ren, B. Xu, J. Du, A. Cao, *J. Polym. Sci., Part A: Polym. Chem.* **2006**, *44*, 3797.
- [21] T. H. Lemmen, E. G. Lundquist, L. F. Rhodes, B. R. Sutherland, D. E. Westerberg, K. G. Caulton, *Inorg. Chem.* **1986**, *25*, 3915.
- [22] C. Jia, S. X. Liu, C. Tanner, C. Leiggenger, A. Neels, L. Sanguinet, E. Levillain, S. Leutwyler, A. Hauser, S. Decurtins, *Chem. Eur. J.* **2007**, *13*, 3804.
- [23] P. J. Skabara, R. Berridge, E. J. L. McInnes, D. P. West, S. J. Coles, M. B. Hursthouse, K. Müllen, *J. Mater. Chem.* **2004**, *14*, 1964.
- [24] C. Jia, S. X. Liu, C. Tanner, C. Leiggenger, L. Sanguinet, E. Levillain, S. Leutwyler, A. Hauser, S. Decurtins, *Chem. Commun.* **2006**, 1878.
- [25] T. Yamamoto, T. Shimizu, *J. Mater. Chem.* **1997**, *7*, 1967.
- [26] D. A. M. Egbe, H. Tillmann, E. Birkner, E. Klemm, *Macromol. Chem. Phys.* **2001**, *202*, 2712.
- [27] M. Besbes, G. Trippé, E. Levillain, M. Mazari, F. L. Derf, I. F. Perepichka, A. Derdour, A. Gorgues, M. Sallé, J. Roncali, *Adv. Mater.* **2001**, *13*, 1249.
- [28] R. Berridge, P. T. Skabara, C. Pozo-Gonzalo, A. Kanibolotsky, J. Lohr, J. J. W. McDouall, E. J. L. McInnes, J. Wolowska, C. Winder, N. S. Sariciftci, R. W. Harrington, W. Clegg, *J. Phys. Chem. B* **2006**, *110*, 3140.
- [29] E. Zhou, C. He, Z. Tan, C. Yang, Y. Li, *J. Polym. Sci., Part A: Polym. Chem.* **2006**, *44*, 4916.
- [30] R. S. Ashraf, M. Shahid, E. Klemm, M. Al-Ibrahim, S. Sensfuss, *Macromol. Rapid Commun.* **2006**, *27*, 1454.
- [31] Y. Xiong, H. Tang, J. Zhang, Z. Y. Wang, J. Campo, W. Wenseleers, E. Goovaerts, *Chem. Mater.* **2008**, *20*, 7465.
- [32] T. Yamamoto, B. L. Lee, *Macromolecules* **2002**, *35*, 2993.
- [33] T. Vahlenkamp, G. Wegner, *Macromol. Chem. Phys.* **1994**, *195*, 1933.
- [34] T. Yamamoto, M. Arai, H. Kokubo, S. Sasaki, *Macromolecules* **2003**, *36*, 7986.
- [35] M. Lanzi, L. Paganin, G. Cesari, *Macromol. Chem. Phys.* **2008**, *209*, 375.
- [36] Naraso, J. Nishida, D. Kumaki, S. Tokito, Y. Yamashita, *J. Am. Chem. Soc.* **2006**, *128*, 9598.
- [37] Naraso, J. Nishida, S. Ando, J. Yamaguchi, K. Itaka, H. Koinuma, H. Tada, S. Tokito, Y. Yamashita, *J. Am. Chem. Soc.* **2005**, *127*, 10142.